energies

MDPI

Article

Simulation of Diesel Engine Properties Using Different Mixtures of Fuels by Means of a Feed-Forward Neural Network: 1. Validation and Prediction of Energetical Parameters

Jonas Matijošius [1,*], Alfredas Rimkus [2], Alytis Gruodis [3], Ornella Chiavola [4] and Erasmo Recco [4]

[1] Mechanical Science Institute, Vilnius Gediminas Technical University—VILNIUS TECH, Plytines Str. 25, LT-10105 Vilnius, Lithuania
[2] Department of Automobile Engineering, Faculty of Transport Engineering, Vilnius Gediminas Technical University—VILNIUS TECH, Plytinės Str. 25, LT-10105 Vilnius, Lithuania; alfredas.rimkus@vilniustech.lt
[3] Faculty of Public Governance and Business, Mykolas Romeris University, Ateities Str. 20, LT-08303 Vilnius, Lithuania; alytis.gruodis@mruni.eu
[4] Department of Industrial, Electronic and Mechanical Engineering, ROMA TRE University, Via Della Vasca Navale, 79, 00146 Rome, Italy; ornella.chiavola@uniroma3.it (O.C.); erasmo.recco@uniroma3.it (E.R.)
* Correspondence: jonas.matijosius@vilniustech.lt; Tel.: +370-68404169

Abstract

This research examines the feasibility of using waste cooking oil (WCO) as a substitute for traditional diesel fuel in internal combustion engines, with a focus on biodiesel production. The aim of this research is to evaluate the effects of WCO–diesel blends on engine performance, with particular emphasis on critical metrics including brake specific fuel consumption (BSFC) and brake thermal efficiency (BTE). The study utilizes artificial neural networks (ANNs) to model and forecast the performance and emission characteristics of engines operating with different fuel combinations. The study employs a methodology that involves conducting experiments to evaluate the mixtures of waste cooking oil (WCO) and diesel fuel in diesel engines. Furthermore, artificial neural networks (ANNs) are employed to develop models for predicting engine performance. The analysis focuses on critical metrics, including BSFC and BTE, under various operating conditions. This research aims to improve sustainable energy solutions by demonstrating the benefits of alternative fuels and advanced artificial intelligence (AI) prediction models in automotive applications.

Keywords: artificial neural network; ANN; data validation problems; engine's emissions; diesel engine

Check for updates

Academic Editor: Diego Luna

Received: 17 January 2026
Revised: 4 February 2026
Accepted: 5 February 2026
Published: 9 February 2026

Copyright: © 2026 by the authors. Licensee MDPI, Basel, Switzerland. This article is an open access article distributed under the terms and conditions of the Creative Commons Attribution (CC BY) license.

1. Introduction

The search for new alternative options for diesel fuel is necessary due to the challenges posed by environmental and economic factors [1]. Diesel combustion releases significant amounts of CO_2, which must be titled as a major greenhouse gas contributing to global warming [2]. Alternative fuels can reduce these emissions, helping to mitigate climate change [3]. Diesel engines spew pollutants like particulate matter (PM) and NOx, which aggravate air quality concerns, including smog and health difficulties [4]. Cleaner alternatives can improve air quality [5]. Diesel fuel comes from petroleum, a finite resource that is becoming increasingly scarce [6]. Diversifying fuel sources reduces dependency on diminishing fossil fuel reserves [7].

Developing alternative fuels drives technological innovation, leading to more efficient and advanced energy solutions [8]. Advances in alternative fuels often promote more

sustainable production practices and the utilization of waste materials, such as waste cooking oil (WCO) for biodiesel [9]. There are several alternative fuels that can replace diesel [10,11]. First, the biodiesel from vegetable oils, animal fats, or recycled greases can be generated by means of transesterification of oils and fats [12]. Biodiesel can be blended with diesel (used in current diesel engines without any modifications). Secondly, using the processes of hydrotreating, renewable diesel (or Hydrotreated Vegetable Oil—HVO) could be produced from fats and oils [13]. From a chemical point of view, HVO is like petroleum diesel.

This work intends to assess the energy and environmental perspectives of diesel and WCO mixtures when used in a conventional diesel engine across a wide range of loads and speeds. Due to weak and very weak correlations between technical, combustion and ecological parameters, a complex assessment can be carried out only with the help of artificial intelligence tools. This article presents a description of engine and simulation techniques and an analysis of energetical parameters. A second article will be dedicated to the analysis of ecological parameters.

The main tasks to be solved are presented below.

1. Engine Performance Assessment. Evaluating the impact of various fuel combinations, namely, WCO, on the performance of traditional diesel engines under varied operating situations. This involves analyzing important factors such as *BSFC* and *BTE*.
2. Application of Artificial Intelligence. Using ANNs to create models and make predictions about engine performance and emission characteristics. These predictions are based on different fuel blends and operating situations. This entails the process of training and verifying ANN models to guarantee their ability to accurately simulate and predict outcomes.
3. Fuel Mixture Optimization. Determining the ideal combinations of diesel and WCO that maximize engine performance while minimizing harm to the environment. This endeavor involves using statistical and AI-driven techniques to enhance fuel composition and engine operating parameters.

This article examines the capacity of alternative fuels to stimulate breakthroughs in diesel engine technology, hence fostering technical innovation and enhancement. This involves examining the incorporation of novel fuels into current engine configurations and discovering possibilities for improving engine efficiency via fuel advancements.

2. Literature Review

2.1. Energetic Problems Related to the Diesel Engine

Using input information, including observed variables and geometric and heat transport characteristics, Payri et al. [14] established thermodynamic diagnosis models that are useful tools for investigating diesel combustion. These parameters can be affected by errors in input parameters, which can be difficult to establish experimentally. The paper investigated the influence of several parameters on the outcomes of a diagnosis combustion model for direct injection diesel engines using a simulated pressure cycle and known input values. Heat transport is shown to be responsive to m_{air} and m_{EGR} but not HR_{max}. For HR_{max}, fuel mass error is small; combustion diagnosis is just marginally susceptible to mbb error. Engine performance and HR_{max} depend on phase angle; injection rate dramatically influences HR_{max}.

Han et al. [15] described the Renormalization Group k–ε (RNG k–ε), hereafter referred to as RNGK-E, developed by Yakhot and Orszag, which has been modified for variable-density engine flows. The model accounts for flow compressibility through isotropic rapid distortion analysis. The modified model is useful for spray combustion modeling, as it

predicts large-scale flow structures affected by spray and squish. The treatment of flow compressibility significantly influences predicted combustion parameters, particularly soot emissions, in diesel engine geometry.

Chakraborty et al. [16] presented the usage of diesel–LPG dual-fuel platforms and artificial neural networks to address environmental concerns and emission regulations. The dual-fuel operation resulted in higher brake thermal efficiency, higher rates of LPG energy share, and lower emissions. The predictive performance of the ANN model was evaluated using the coefficient of determination (R^2), root mean square error (RMSE), and mean absolute percentage error (MAPE), which together provide correlation-based and error-based measures of model accuracy. The results show a perceptible increase in brake thermal efficiency, energy consumption rates, and exhaust temperature rise. The dual-fuel platform also shows a reduction in NOx emissions, unburnt hydrocarbons, soot emissions, and CO emissions. The study concludes that the artificial neural network can accurately imitate engine performance and emission characteristics in diesel–LPG dual-fuel platforms.

Gul et al. [17] maximize the fuel type, engine speed, and load for a DI-CI diesel engine by use of the L9 (33) Orthogonal Array (OA) of the Taguchi design. Waste cooking oil-based pure biodiesel (B100) fuels the engine, together with a 20% blend of biodiesel with neat diesel (B20). Reducing smoke and NOx emissions as well as enhancing engine performance are the aims. With a 44.28% effect on output characteristics, the study reveals that the kind of fuel is the most affecting element. The work confirms the application of the Grey–Taguchi technique in concurrently lowering emissions and enhancing combustion and performance. Saving engineering work and expenses, the study also reveals that the ANN approach may be effectively applied to evaluate emission, combustion, and performance traits of I.C engines.

Using an artificial neural network (ANN) and Support Vector Machine (SVM), Niu et al. [18] examine their predictive accuracy for response prediction in a common rail direct injection system (CRDI)-assisted marine diesel engine. The work compares the performance of the ANN and SVM by training data using the Taguchi orthogonal array. With little experimental data, SVM shows outstanding predictive accuracy and generalization ability; the ANN may converge to a local minimum and encounter overfitting difficulties. The paper claims that SVM may greatly lower experimental costs and is ideal for diesel engine response predictions. Nevertheless, by adjusting starting weights and threshold values, one can increase the stability and accuracy of the ANN; so, future research should concentrate on parameter optimization for SVM and ANNs.

The work by Bhowmik et al. [19] investigated how oxygenated fuel affects the performance and exhaust emissions of a diesel engine running on contaminated diesel. An artificial intelligence (AI)-based artificial neural network (ANN) model was developed to forecast outputs, including brake thermal efficiency, brake specific energy consumption, oxides of nitrogen, unburned hydrocarbons, and carbon monoxide. The model was found to be strong and relevant in Diesosenol platform engine output prediction. The ideal engine running conditions were also found using Multi-Objective Response Surface Methodology (MORSM). With values of R, MSE, and MAPE spanning 0.999312 to 0.999852, the accuracy of the ANN model was found to match experimentally measured outputs. Using the MORSM model, the research also created a very good diesel engine performance–exhaust fume trade-off spectrum. Closely matched and tested in the same experimental engine, the optimal values of load and mixture concentration revealed that a higher ethanol share in adulterated diesel fuel could raise the diesel supplementation ratio and lower exhaust emissions [20].

Gholamian et al. [21] study a very efficient fuel cell (FC) system coupled with a vanadium chlorine scheme and a Stirling engine. The system is assessed in technical,

financial, and environmental spheres. The ideal solution point is found by a machine learning-based gray wolf algorithm optimization approach. With a ζ equal to 0.21, the TOPSIS point corresponds with the maximum efficiency and hydrogen generation of 81% and 0.008 kg/s. At the TOPSIS point with a levelized cost of 0.14 $/kWh, the maximum net power generation and hydrogen production take place. Furthermore, the study shows the SOFC's maximum exergy destruction rate and the growing efficiency and net output power resulting from a 100 °C cell temperature [22].

Hoang et al. [23] presented an ANN model that has emerged as a promising approach to predict engine performance and exhaust emissions in the context of biodiesel, a promising biofuel. This model, which combines artificial neural networks (ANNs) with trained, tested, and validated data, has shown high accuracy in predicting engine behaviors with an accuracy of over 95%. ANNs work similarly to the human brain, utilizing interlinked neurons to manage data and learn from transactional relationships. The model's performance is predicated on a performance function (MSE), honed by error weights. The approach of training is a feed-forward back-propagation network. Because they learn the relationship between controlled/unlimited variables and input parameters, ANN models investigate previously recorded data and are faster than conventional simulation tools and mathematical models. Predicting the ideal condition in the core correlation of inputs and outputs, as well as optimizing engine performance and emission characteristics driven with biodiesel-based fuels, depends critically on the ANN model [24,25]. However, the back-propagation algorithm, with its slow gradient descent, may require further development for practical problems. Future algorithms based on standard numerical optimization could be more effective in predicting engine performance and emissions.

Castresana et al. [26] examined the reliability of artificial neural networks in predicting various performance and emission metrics for a marine diesel engine. The artificial neural network underwent training and validation using a dataset comprising 1000 samples, subsequently being evaluated across various operational points of a six-cylinder marine diesel engine. The mean absolute percentage error (MAPE) values remained under 8.5% for all parameters, apart from predictions related to CO and NO_2 emissions. In the analysis of low-temperature and high-temperature cooling systems, oil systems, and exhaust gas systems, the MAPE values were recorded to be under 4.3%. The computation duration for 24 test samples, each containing 35 parameters, was recorded at 0.109 s. This demonstrates the ANN's ability to predict multiple outputs with notable efficiency in processing time.

The research findings indicate that artificial neural networks are capable of predicting 35 parameters derived from randomly chosen points on the engine performance map, with mean absolute percentage error values falling below 8.5%. Remarkable precision was noted in systems involving low- and high-temperature water, oil, and exhaust gases. The ANN exhibits a remarkable ability to generalize, even when functioning in previously unexplored regions of the engine performance map, thereby affirming its role as a reliable and effective tool for real-time modeling applications. Future research endeavors may adopt this modeling approach to discern anomalies and uncover faults within systems.

Uslu et al. [27] conducted a thorough evaluation of the efficacy of two distinct modeling methodologies, namely, an ANN model and an RSM model, in predicting engine performance and emission characteristics of palm oil–diesel blends. The RSM model exhibited superior predictive accuracy, as indicated by significant R^2 values, while the ANN model showed R^2 values between 0.88 and 0.95. The optimal operating parameters for the RSM model were identified as a palm oil percentage of 17.88%, an injection advance of 35 °C CA, and an engine capacity of 780 watts. The RSM model produced more accurate results compared to the ANN model in the estimation of engine outputs. The study highlighted the importance of RSM in assessing the impact of different variables on engine

performance and exhaust emissions. The RSM model demonstrated benefits in predicting and improving engine performance and emission metrics.

2.2. ANN for Simulation Engine Properties

Noor et al. [28] employ an artificial neural network (ANN) model to forecast engine performance metrics, such as output torque, brake power, brake specific fuel consumption, and exhaust gas temperature. The artificial neural network model, constructed through the application of a standard back-propagation Levenberg–Marquardt training algorithm, exhibited remarkable precision, achieving a coefficient of determination (R^2) of 0.99, thereby surpassing the performance of the mathematical model [29].

Jeon et al. [30] propose an accurate regression model for fuel consumption in smart ships using an ANN through big data analysis. The model employs a range of concealed layers, neurons, and activation functions to forecast fuel consumption, rendering it superior in accuracy and efficiency compared to polynomial regression and support vector machines.

Yusaf et al. [31] use ANN modeling to predict brake power, torque, *BSFC*, and exhaust emissions of a modified diesel engine. The ANN model predicts better engine performance and emission characteristics when using a combination of CNG and diesel fuel. The standard back-propagation algorithm is used for training, and a multilayer perception network is used for nonlinear mapping. The ANN model provides an accurate and simple analysis and simulation of engine parameters, making it a useful tool for evaluating engine parameters.

Ahmad et al. [32] described energy prediction models that are crucial for building performance evaluation, enhancing energy efficiency and decision-making by facility managers and utilities. Their research examined the efficacy of feed-forward back-propagation artificial neural networks and random forest algorithms in predicting HVAC energy consumption within a hotel located in Madrid, Spain. The ANN exhibits a slight improvement, achieving a root mean square error (RMSE) of 4.97 compared to 6.10. Nonetheless, algorithms that utilize ensemble methods present a distinct advantage when addressing the intricacies of multi-dimensional data, which is characteristic of architectural structures. The random forest algorithm conducts internal cross-validation through the utilization of out-of-bag samples and encompasses several tuning parameters. Both models exhibit similar predictive capabilities and are nearly equally relevant in the context of building energy applications.

Within the realm of built environment research, ensemble-based methodologies, including random forest, have frequently been overlooked, notwithstanding their considerable promise. Random forests have been developed to address the limitations inherent in classification and regression trees (CARTs), which are prone to producing unstable models and exhibit considerable variability in their variables. Random forests can manage high-dimensional datasets, executing internal cross-validation, and possess several tuning parameters. The constructed model will enhance comprehension of intricate data, discern patterns, evaluate hypothetical scenarios, and assist energy managers and building proprietors in making well-informed decisions.

Cirak et al. [33] used an ANN model to predict the torque of a diesel engine using biodiesel produced from canola and soybean oils through transesterification. The model was trained using Levenberg–Marquards algorithms and tested on a four-cylinder and four-stroke test engine. The results showed that the ANN model accurately predicted engine performance, with a correlation coefficient of 0.98 for engine torque and an MSE error of 0.0002. The ANN results were found to be very good, with acceptable values and low root mean square errors, demonstrating the effectiveness of ANNs in solving engineering problems.

Bizon et al. [34] examined, in detail, the process of designing and optimizing reliable artificial neural networks (ANNs) for the diagnostics of a three-cylinder diesel engine under various operating conditions. The study used a radial basis function (RBF) neural network, the performance of which was evaluated using data not included in the training sample. The results obtained showed high accuracy in predicting pressure signals and derived engine parameters; therefore, this method is suitable for use in closed-loop engine control systems. The RBF neural network is considered a promising solution for serial production vehicles, as it allows diagnostics without invasive and expensive measurement probes.

Kokkullunk et al. [35] analyzed the impact of exhaust gases on human health and the environment, emphasizing the need for strict regulation of these pollutants. The International Convention for the Prevention of Pollution from Ships (MARPOL) addresses the problem of marine pollution by setting emission limits. In MARPOL-defined Emission Control Areas (ECAs), emissions must be controlled with extreme care. Direct injection (DI) diesel engines are widely used as a propulsion system for marine vehicles, but predicting and controlling their emissions in real time remains a challenging task. In their study, an artificial neural network framework based on the back-propagation algorithm and the radial basis function method was developed to predict emissions and exhaust gas temperatures in DI diesel engines using emulsified fuel. A comparative analysis of the results of the BP and RBF networks with experimental data obtained from real diesel engine tests was presented. The results of the study showed that both ANN models have high accuracy, but the RBF network demonstrated greater reliability.

Diesel engine exhaust emissions, especially of the direct injection (DI) type, pose a significant threat to the environment and human health. The MARPOL Convention regulates the amounts of these pollutants, and strict limit requirements are set in Emission Control Areas (ECAs). In their study, an ANN framework was developed to predict emissions and exhaust gas temperature in DI diesel engines using emulsified fuel. The model results were compared with real diesel engine experimental data.

Selvaraj et al. [36] described various improvements in waste cooking oil (WCO) blends. Fatty acid methyl esters (FAMEs) were obtained from waste cooking oil by direct transesterification using methanol. The WCO was pretreated using 1% potassium methoxide as a catalyst and 2% activated carbon as an adsorbent. The Box–Behnken response surface methodology was used in conjunction with an artificial neural network model to optimize the process variables of biogas production. The highest conversion rate of 95% was achieved under optimal conditions, with determination coefficients of R^2 of 0.98 for the RSM model and 0.99 for the ANN model. The composition of FAME was studied in detail using ^{1}H NMR, ^{13}C NMR, FT-IR spectroscopy and gas chromatography–mass spectrometry (GC–MS). It was found that the acidity of FAMEs was lower than that of standard diesel, indicating the suitability of this fuel for a short-term conversion process using microwave technology.

Tütüncü et al. [37] performed a comprehensive analysis of the performance and emission characteristics of internal combustion engines fueled by diesel and gasoline using artificial neural networks. ANN models were used to model various engine parameters such as air flow, injection pressure, fuel consumption, duty cycle and load. The determination coefficient values related to torque, power, specific fuel consumption and emission parameters were analyzed. The simulation results were compared with experimental data, which showed that the dynamic load value was suitable for modeling the performance and emissions of diesel engines. The study also revealed high predictive values for both types of engines compared to previous studies.

Oğuz et al. [38] applied artificial neural networks in the automotive sector to predict engine performance using various biofuels, including biodiesel, bioethanol and biogas. An

ANN model was developed to estimate power, torque, fuel consumption and specific fuel consumption. The model was extensively tested using diesel, biodiesel, B20 blends and bioethanol–diesel blends, taking into account different fuel compositions and properties. The results obtained showed an extremely high reliability of 99.94%, and the correlation coefficients approached 1, indicating a very good agreement between the ANN predictions and experimental measurements. The study did not find significant differences between the modeled and experimental results, which confirmed the reliability of the method and its potential to reduce testing costs, time and labor.

Carbot-Rojas et al. [39] conducted a comprehensive review of the development of internal combustion engines, focusing on modeling methods, biofuel use, control system design, and maintenance systems. The models were divided into linear, nonlinear, and neural network-based models. Biofuels used in internal combustion engines included pure biofuels, such as ethanol, methanol, and hydrogen, as well as gasoline–alcohol blends and their combinations with hydrogen additives. The classification of control systems depended on the approach used and included model-based, observer-based, and intelligent control. Fault diagnosis methods were developed to detect sensor or equipment malfunctions. The increasing attention to biofuels is associated with the limitations of fossil fuels and pollution problems. The studies analyzed the effects of biofuels on engine performance and NOx emission reduction. The development of advanced materials and coatings is considered a promising tool for reducing corrosion in engines. Future research could focus on developing model-based fault-tolerant control systems using either active or passive approaches.

Lehn et al. [40] focused on developing quantitative structure–property relationship (QSPR) models for predicting the research octane number (RON), the motor octane number (MON), and octane sensitivity (OS) for individual fuel components. The models were developed based on experimental RON and MON data covering 260 pure fuel components, both oxygen-free and oxygenated hydrocarbons. A backward feature elimination method was used to reduce the number of input variables, which showed that the OS model required fewer input parameters than the RON and MON models. Sensitivity analysis provided valuable insights into the influence of input features on the predicted quantities. The study confirmed that artificial neural networks are highly effective in accurately estimating the antiknock properties of fuel compositions, and the appropriate selection of input variables based on physical knowledge is essential for the accuracy of the model. This opens up the possibility of applying analogous methods to predict other fuel parameters, such as ignition delay time or flame propagation velocity.

López-Flores et al. [41] presented a new multi-objective methodology for the utilization of waste heat flows and energy integration between heat engines and industrial facilities. The methodology combined pinch analysis, mathematical models, machine learning systems and optimization algorithms. The analyzed heat engines included the steam Rankine cycle, the organic Rankine cycle and the absorption refrigeration cycle, for which multilayer perceptron neural networks were used to model them. The non-dominated solution genetic algorithm NSGA-III was used to solve the optimization problem. The methodology comprehensively examined the trade-offs between economic, environmental and social factors [42]. The analysis confirmed the significance of the proposed method, and the optimal parameters of the MLP models were determined experimentally, achieving high prediction accuracy. The optimization results showed that different MLP networks related to heat engines can be successfully integrated into a common model of industrial waste heat utilization systems. The proposed methodology is characterized by high versatility and can be applied to various practical cases.

2.3. Combustion Characteristics of Diesel Engines Using Fuel Mixtures

The combustion process in diesel engines is greatly affected by the physical and chemical characteristics of the fuel, particularly when utilizing blends with alternative or oxygenated fuels. Literature reviews show that fuel density, viscosity, cetane number, oxygen content and lower heating values directly affect the characteristics of fuel atomization, ignition delay, heat release rate and overall combustion efficiency [43].

Experimental studies involving biodiesel and diesel blends (e.g., B20, B50) indicate that combustion and emission characteristics are significantly influenced by the fuel mixture's composition and the combustion control strategies employed, including fuel injection timing and multi-stage injection. It has been found that properly selected combustion strategies allow for simultaneous reduction in NOx and particulate emissions while maintaining acceptable thermal efficiency [44].

Oxygenated fuels and their blends often exhibit shorter ignition delays and altered heat release characteristics. This results in a decrease in carbon monoxide, hydrocarbon, and particulate emissions; however, in certain situations, specific fuel consumption may increase due to a lower fuel heating value [45]. Reviews also confirm that in the case of biodiesel and diesel blends, BSFC usually increases, while BTE may decrease slightly or remain similar, depending on load and engine mode [46].

Ignition delays and heat release rates are crucial for combustion processes. Studies show that the use of biodiesel and its blends usually shortens the ignition delay, reduces the maximum cylinder pressure and changes the distribution of heat release phases [47]. Meanwhile, fuels with a higher oxygen content promote more efficient combustion and soot oxidation, but they cause nonlinear relationships between combustion parameters and engine operating conditions [48].

Observational and numerical studies confirm that the combustion processes of blends are characterized by a complex, weakly correlated dependence between input and output parameters; therefore, traditional regression methods are often not sufficient for accurate prediction [49]. For this reason, data-driven methods are increasingly being used, but it is emphasized that their reliability directly depends on the choice of input variables reflecting the physical basis and the quality of experimental data.

In this regard, this work examines diesel and WCO mixtures by integrating fuel properties and engine operating parameters characterizing the combustion process, in order to ensure that the subsequently applied artificial neural network models are based on real combustion processes and not just on statistical relationships.

3. Materials and Methods

3.1. Experimental Equipment and Materials (Fuels)

Experimental studies were carried out using a water-cooled two-cylinder diesel engine equipped with a common rail fuel injection system. The design and operating parameters of the engine are summarized in Table 1. To ensure the load and operating modes, the engine was mechanically connected to an asynchronous electric motor, Siemens 1PH7, whose rated torque is 360 nm and rated power is 70 kW. The mentioned engine was affixed within the testing apparatus of the Engineering Department at Roma Tre University. The torque measurement was conducted utilizing an HBM T12, a strain gauge transducer that incorporates an optical encoder. The AVL Fuel Balance 733 apparatus was employed to quantify fuel consumption. The in-cylinder pressure was measured utilizing a piezoelectric transducer identified as AVL GU13P.

Table 1. Technical details of the engine.

Engine Type	Common Rail, Naturally Aspirated, Water Cooled
Cylinders	2
Displacement	440 cm^3
Bore	68 mm
Stroke	60.6 mm
Compression ratio	20:1
Maximum power	6.7 kW @ 3600 rpm
Maximum torque	20 nm @ 2400 rpm

The rotational velocity of the engine was quantified utilizing an angular sensor (AVL 364C) that generates 2880 pulses per revolution.

The fuel properties were determined by assessing the properties of pure diesel and pure WCO (Table 2). The fuel blends were mixed by adding 20% and 40% WCO by volume to diesel. The fuel blends were mixed with 20% and 40% WCO by volume added to the diesel, but the mass fraction of the individual components of the mixture was used to assess the fuel properties. The augmentation of WCO concentration within the mixture results in an elevated C/H ratio and a heightened oxygen concentration; however, it concurrently diminishes the lower heating value. Each of these factors significantly influences the combustion process and the overall energy efficiency of the engine.

Table 2. Main properties of the fuels tested.

Label	Unit	WCO0	WCO20	WCO40
Volume fraction of WCO	%	0	20	40
Volume fraction of diesel	%	100	80	60
Density	$kg{\cdot}m^{-3}$	822.5	833.4	844.3
Carbon/hydrogen ratio (C/H)	-	6.80	7.90	8.99
Lower heating value (LHV)	$MJ{\cdot}kg^{-1}$	43.33	42.0	40.74
Volumetric O_2 concentration in fuel	%	0.2	2.465	4.885
Stoichiometric air to fuel ratio (l_0)	1 kg of air/1 kg of fuel	14.53	13.85	13.18
Cetane number (CN)	-	55	55.2	55.4

3.2. Data Collection

Table 3 delineates the array of experimental parameters pertaining to the diesel engine employed as input for the artificial neural network. Ten parameters (K01, ..., K10) represent the input layer suitable for simulation.

Table 3. Experimental parameters of the diesel engine utilized for the ANN as input parameters.

Index	Abbr.	Parameter	Units	Interval	
				X_{MIN}	X_{MAX}
0	K01	Brake mean effective pressure $(BMEP)$	MPa	0.2	0.7
1	K02	Engine speed (n)	rpm	2000.0	4000.0
2	K03	Volume fraction of WCO	-	0.00	1.00
3	K04	Volume fraction of pure diesel	-	0.00	1.00
4	K05	Density	$kg{\cdot}m^{-3}$	820.0	850.0
5	K06	LHV	$MJ{\cdot}kg^{-1}$	40.0	44.0
6	K07	C/H ratio	-	6.0	9.0
7	K08	Volumetric O_2 concentration in fuel	%	0.0	5.0
8	K09	Stoichiometric air-to-fuel ratio (l_0)	1 kg of air/1 kg of fuel	13.0	15.0
9	K10	CN	-	55.0	56.0

Table 3 delineates the array of experimental parameters pertaining to the diesel engine employed as input for the artificial neural network. Ten parameters (K01, ..., K10) represent the input layer suitable for simulation.

Table 4 presents a list of experimental parameters of the diesel engine used for the ANN as output. In the output layer, two energy parameters (L08, L09) and the excess air rate (L01) are given. The excess air ratio (λ) is not a direct indicator of energy but provides additional information on engine operating conditions and the composition of the air/fuel mixture.

Table 4. Experimental parameters of the diesel engine utilized for the ANN as output parameters.

Index	Abbr.	Parameter	Units	Interval	
				Y_{MIN}	Y_{MAX}
0	L01	The excess air ratio (λ)		1.0	3.0
7	L08	Brake specific fuel consumption (*BSFC*)	$g \cdot kWh^{-1}$	200	350
8	L09	Brake thermal efficiency (*BTE*)	-	0.2	0.4

Table 5 presents the sets of events for simulation. Three different mixtures of fuels were used for the experiment: (i) pure diesel (labeled WCO0), (ii) a mixture containing 80% of diesel and 20% of WCO (labeled WCO20), and (iii) a mixture containing 60% of diesel and 40% of WCO (labeled WCO40)—see Table 2. To check different loads and speeds in large intervals, several working regimes were used. Load 100% was used for pure diesel only, and loads 80%, 70%, and 50% were used for WCO0, WCO20, and WCO40. In all cases, speed *n* (in rpm) was distinguished as 2400, 2700, 3000, 3300, and 3600. Set00 was formed from events 0–19 (for WCO0 pure diesel, including loads 100%, 80%, 70%, and 50%). Set-002040 was formed from events 1–3, 5–7, 9–11, 13–15, 17–19, and 20–49 (for WCO0, WCO20, WCO40, includes loads 80%, 70%, and 50% only; load 100% is absent). Two sets, namely, set00 and set02040, were used for validation only. Joint set Set-total (events 0–49, used for learning purposes) was formed as the union of set00 and set02040.

Table 5. Sets of events.

Simulation Sets			Parameter	Fuel Properties and Machine Regime			
Experimental events	File	Set name	Fuel	Pure diesel	Pure diesel	Diesel + B20	Diesel + B40
			Load, %	100	80, 70, 50	80, 70, 50	80, 70, 50
			Speed *n*, rpm, K02	2400, 2700, 3000, 3300, 3600	2400, 2700, 3000, 3300, 3600	2400, 2700, 3000, 3300, 3600	2400, 2700, 3000, 3300, 3600
0–19	200.txt	Set-00		+	+	−	−
1–3, 5–7, 9–11, 13–15, 17–19, 20–49	202.txt	Set-02040		−	+	+	+
0–49	111.txt	Set-total		+	+	+	+

3.3. Validation

To support the implementation of the proposed ANN model, the VALLUM01 software package was developed. This tool provides a structured environment for defining the neural network architecture, data normalization procedures, and training control. Within this framework, a feed-forward neural network with a single hidden layer was implemented, as described below.

Simulations were provided using a desktop computer Intel (R) Core (TM) i5-6400 CPU @ 2.70 GHz, RAM 8 GB. The operating system was Windows10Pro, version 22H2. The advanced tool *VALLUM01* [50], as an implementation of an artificial neural network (ANN) (containing two classes: Neural_Network and Matrix [51]), was described previously [52–55]. Table 6 represents the parameters of the ANN simulations. A schema of the feed-forward neural network (FNN) is presented in Figure 1. Two distinct plugins were employed for the conversion of data from any real interval to a fuzzy logic interval (0; 1), facilitating both forward and backward transformations for input and output purposes. The main functionality of the VALLUM01 tool is the implementation of a feed-forward neural network (FNN), which consists of an input layer, a single hidden layer, and an output layer. Quantities of the input/output layers are presented in Figure 1. The hidden layer consists of the requested number of perceptrons Q = (100, 200). As a result of the adjustments made, bias was incorporated into the hidden layer.

Table 6. Parameters of ANN simulations.

Behavior or Parameter	Name or Value
Realization of ANN	Feed-forward neural network (FNN)
Package name	*VALLUM01*
Architecture of ANN	FNN containing a single hidden layer
Nonlinear function	Sigmoid
Input layer	Number of units P = 11
Hidden layer	Number of perceptrons Q = 100, 200
Output layer	Number of units R = 3
Learning rate	0.01
Optimization algorithm	Gradient descent
Training interval	Number of epochs until 300,000,000
Training until escape	Number of epochs 249,734,963
Escape parameter for the end of training	$TNE^2 < 9.8 \times 10^{-8}$
Training amount	Number of observations (events) N = 50
Validation amount	Number of observations (events) N = 50

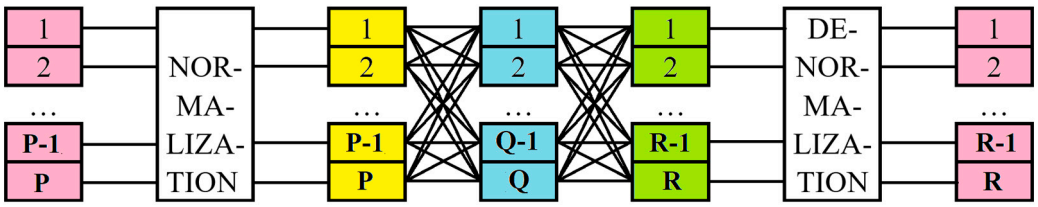


Figure 1. Illustration of an artificial neural network (ANN): the input layer is composed of P = 11 units (yellow), a single hidden layer includes Q = (100, 200) perceptrons (blue), and the output layer consists of R = 3 units (green). Normalization and denormalization plugins are utilized to transform any real value (pink) from the designated interval into the (0; 1) interval. Routine operations are executed sequentially from left to right. Data flows from left to right.

The programmed package *VALLUM01*, which features a graphical user-friendly interface for input, output, and control, was developed utilizing the JAVA *Eclipse* framework. In the context of the ANN, two representative classes from [51] were employed: *Matrix* and *NeuralNetwork*. The nonlinear sigmoidal function was employed as the activation function. Prior to training, the input and output data were normalized to ensure numerical stability. Subsequently, the training process was performed using the gradient descent optimization algorithm:

$$\sigma(x) = \frac{1}{1 + e^{-x}} \quad (1)$$

3.4. Organization of Data Input/Output

The data conversion plugin (normalization/denormalization; refer to Figure 1) recalibrates the experimental input values X_i (i= 0; P) and output values Y_j (j = 0; R) to their respective fuzzy logic values XX_i, YY_j in either the forward or backward direction, in accordance with the specified formulas:

$$XX_i = \frac{X_i - X_{MIN}}{X_{MAX} - X_{MIN}}, \quad (2)$$

$$X_i = X_{MIN} + XX_i(X_{MAX} - X_{MIN}). \quad (3)$$

where X_{MIN} and X_{MAX} denote the minimum and maximum values of the dataset X_i (i= 0; P), respectively. After calibration, XX_i values are presented in the interval (0, 1).

4. Results

4.1. Experimental Regimes

Table 6 illustrates the distribution of the experimental event, specifically the current operational state of the diesel engine, in relation to the various technical regimes numbered from 0 to 50. Experimental testing was conducted with the engine operating at various speeds and loads, adjusting the exhaust gas recirculation (EGR) and the start of injection (SOI) in accordance with the control algorithm supplied by the engine control units.

In the I stage, pure diesel fuel without any WCO additions was used (conditional fuel name WCO0). In the II stage, WCO 20 (mixture consisting of 80% diesel by volume and 20% WCO by volume) was used. In the III stage, WCO40 (mixture consisting of 60% diesel by volume and 40% WCO by volume) was used.

For the pure diesel tests, the engine was loaded to 100%, 80%, 70% and 50% of nominal load at different engine speeds (2400 rpm, 2700 rpm, 3000 rpm, 3300 rpm and 3600 rpm). Using diesel and WCO blends, the engine was not able to develop its nominal power, so during the test, the engine was loaded with three loads (80%, 70% and 50%) at five different engine speeds (2400 rpm, 2700 rpm, 3000 rpm, 3300 rpm, and 3600 rpm). The power output of the engine was reduced because the lower heating value of the fuel mixture was reduced, and the fuel injectors were not able to provide the higher fuel quantity needed to achieve the required power.

Figure 2 delineates the methodologies employed for the training and validation of the artificial neural networks. The parameters are delineated in accordance with the notation illustrated in Figure 1. At the outset, the training data file 05_17.csv was created in its original form. The training procedure was requested for E = 100,000,000 epochs and E = 300,000,000 epochs for an artificial neural network comprising a single hidden layer with M = 100 and M = 200 perceptrons, respectively, across two distinct training projects, aa6 and aa8. The key parameter for management of the training interruption process is Total Network Error (TNE), obtained using Formula (4)

$$TNE^2 = \frac{1}{N}\sum_{i=1}^{N}\left(X_i^{current} - Target_i^{fix}\right)^2 \quad (4)$$

The target value is obtained from the experiment, and the current value is obtained in simulations at each epoch. N represents the number of observations (events). In both training projects, training was interrupted when the value of TNE^2 exceeded the values 5×10^{-7} and 1×10^{-7}, respectively. Exact values of E and TNE^2 are presented in Table 7. Using the presented routine, training stamps 100-05_17 and 200-111 (corresponding to 05_17.csv and 111.csv, respectively) were obtained. Then, for the validation procedure, the same file, 111.csv, was used in the prediction regime, together with the training stamp

200-111 only. Table 6 presents the evolution of the ANN training in the form of TNE^2 dependence on the epoch number.

Table 8 shows the evolution of the training process of an artificial neural network (ANN) using different numbers of perceptrons per hidden layer (Q) over a certain number of epochs. The top graph shows the ANN training with 100 perceptrons, in which the squared Total Network Error (TNE^2) decreases, indicating progress in network learning and a reduction in errors. Training was terminated when an error threshold of $4.96 \cdot 10^{-7}$ was reached after 79,866,326 epochs. The bottom graph, representing training with 200 perceptrons, also shows a decreasing trend in error, but the final error value is lower ($9.54 \cdot 10^{-8}$) after 249,734,963 epochs. This suggests that a larger number of perceptrons can help the network learn more accurately. In general, both graphs demonstrate how the squared error value decreases with an increasing number of epochs, indicating the improvement in the network and increasing accuracy with a higher number of perceptrons.

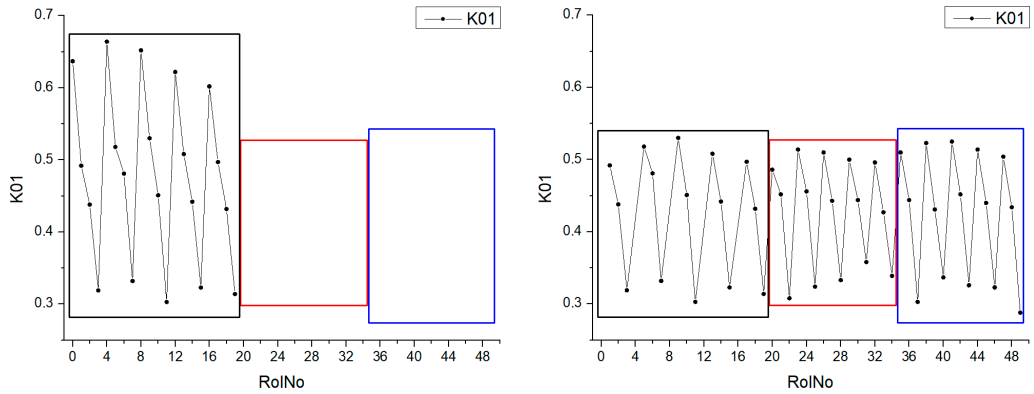


Figure 2. Experimental events (0, . . ., 50) of the diesel engine. Events are related to the different technical regimes labeled using the input *BMEP* (K01 parameter). Black, red, and blue colors represent the use of WCO0, WCO20, and WCO40 fuels (I, II, and III stages), respectively.

Table 7. The methodology involved the training and validation of artificial neural networks. The input layer consists of $P = 11$ units, while the output layer comprises $R = 3$ units. The single hidden layer contains Q perceptrons, with a learning rate set at 0.01 and a specified number of training epochs denoted as E.

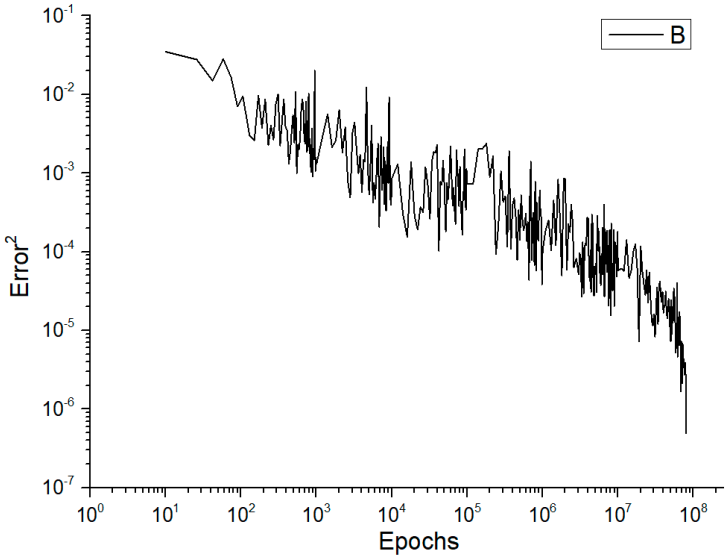
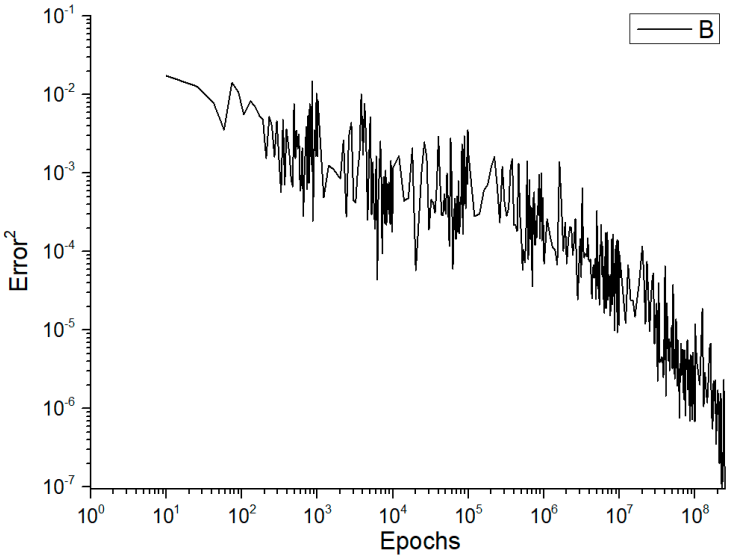
Project	**The Quantity of Perceptrons in the Singular Hidden Layer**	**Training**					**Validation**	
Name	Q	Data file	Exp. Events	Epochs, E	TNE^2	Chart	Data file	Exp. Events
aa6	100	05_17.csv	50	79,866,326	$4.96 \cdot 10^{-7}$	Table 8		
aa8	200	111.csv	50	249,734,963	$9.8 \cdot 10^{-8}$	Table 8		
aa8	200	111.csv					200.csv	20
aa8	200	111.csv					202.csv	30

4.2. Distributions of Energetical Parameters

Table 9 displays graphs illustrating the experimentally determined results of the excess air ratio (λ) in two datasets, Set-00 and Set-02040. The graphs also provide a comparison between the actual data and the model projections. The upper graphs indicate that both datasets, L01 (actual data) and L01* (model predictions), exhibit comparable variations. However, Set-00 displays a wider range of fluctuations, while Set-02040 demonstrates more frequent and consistent fluctuations. The lower graph displays the alignment between the model's predictions and the observed data, demonstrating a high level of accuracy in both

instances, as seen by the tight correspondence between the forecasts and the actual data. This indicates that the model consistently replicates the surplus air ratio values in both scenarios, showing a high level of prediction accuracy.

Table 8. The dependence of TNE^2 on the number of epochs. The progression of training methodologies for artificial neural networks. A total of 50 events was recorded. The quantity of perceptrons present within the singular hidden layer *Q*. The training process was halted upon surpassing the specified threshold for TNE2. The escape value associated with the realized training epochs *E* was derived.

Q	TNE^2	*E*	
100	4.96×10^{-7}	79,866,326	
200	9.54×10^{-8}	249,734,963	

The excess air ratio helps to evaluate combustion conditions. Combustion quality worsens when the excess air decreases and there is insufficient oxygen, which is necessary for the oxidation of the hydrocarbons contained in the fuel. However, too much excess air also reduces the energy efficiency of combustion by generating less power. In Table 7, we can see that the excess air decreases when the load is reduced, but this indicator also decreases when the engine speed is increased because the volumetric efficiency of the engine decreases due to increasing air flow resistance. Increasing the WCO concentration to 20% results in a slight increase in excess air, as these fuel mixtures contain more oxygen. The

C/H ratio also increases, and carbon oxidation requires less oxygen compared to hydrogen oxidation. However, when the WCO concentration is increased to 40%, the excess air does not increase further, which is probably due to the higher mass of the injected fuel.

Table 9. Comparison of the λ meaning using experimental data and simulation.

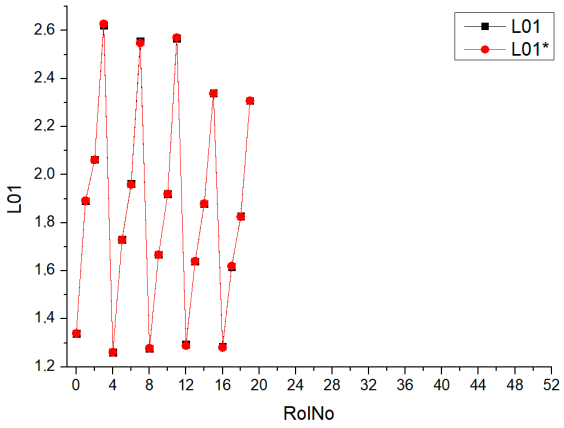
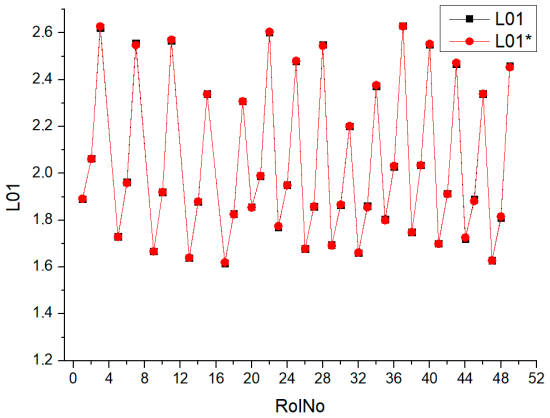
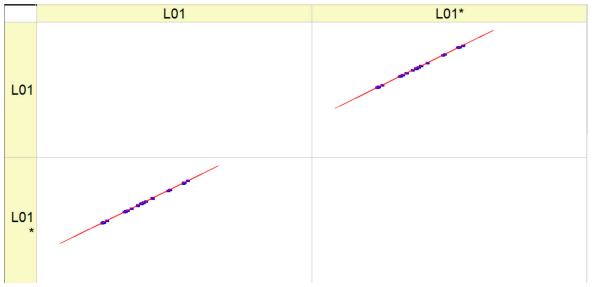
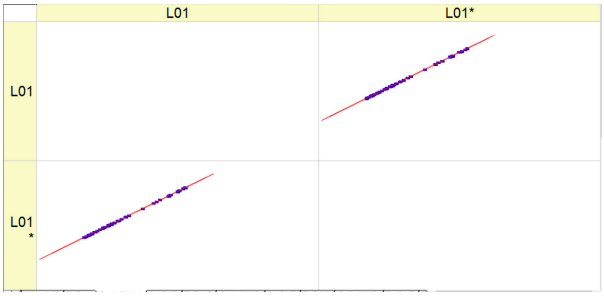
Set-00	Set-02040
	
	

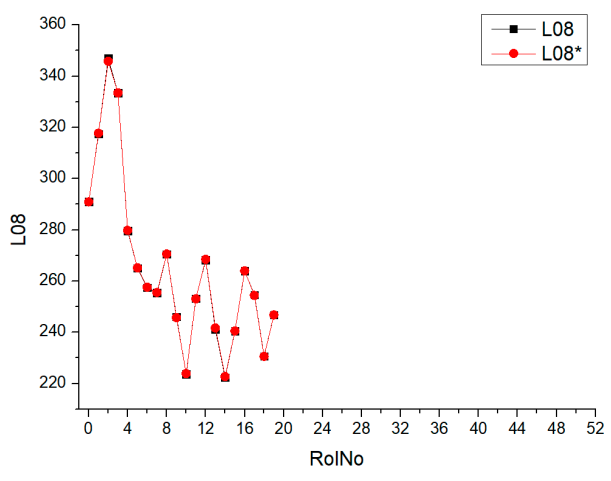
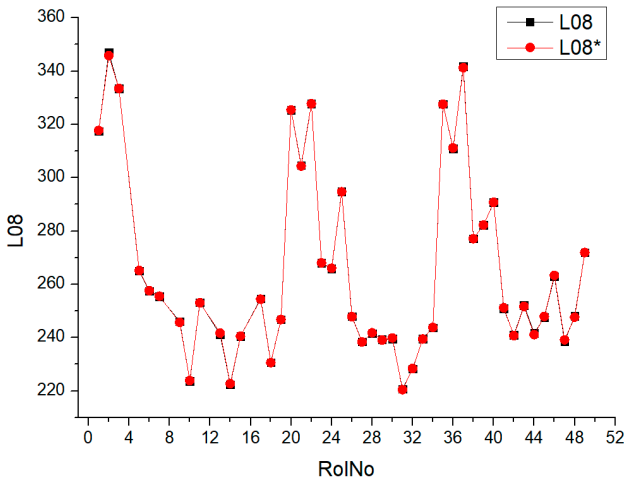
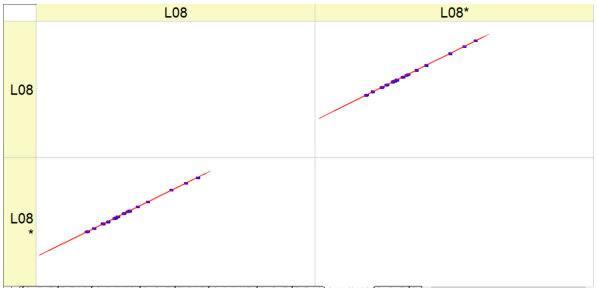
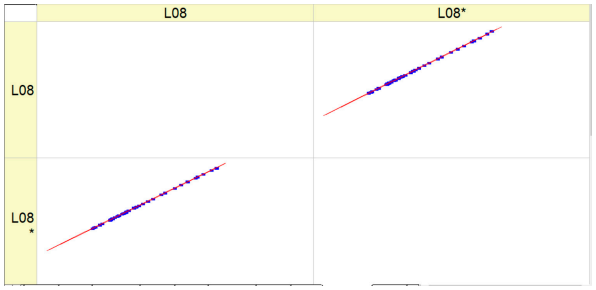
Table 10 displays graphs illustrating the measurements of *BSFC* for two sets of data, namely, Set-00 and Set-02040, along with their comparison to model projections. Set-00 has a conspicuous downward trend, declining from around 360 g/kWh to about 220 g/kWh, indicating a significant decrease in fuel usage throughout the trials. Meanwhile, in Set-02040, the changes in *BSFC* are more diverse and less uniform, suggesting a higher degree of variance in costs across various trials. The lower plots illustrate the tight correspondence between the model predictions (L08*) and the actual data (L08), confirming the model's great accuracy in predicting precise fuel use. This is evident from the points when the model's predictions and the actual data come together, indicating that the model effectively adjusts to real-world circumstances. The congruence between the model and the empirical data affirms the dependability of the model in forecasting *BSFC* values, notwithstanding the distinct characteristics of oscillations in the two datasets.

Different trends of *BSFC* variation are observed with different engine operating modes and with different fuel mixtures (Table 10). The lowest specific fuel consumption using pure diesel was achieved with the engine operating at 70% load and 3000 and 3300 rpm. Similarly good fuel consumption results were achieved with WCO20 fuel mixture at 70% engine load at 3300 rpm. A further increase in WCO concentration resulted in an increase in *BSFC*.

Table 11 displays the outcomes of measurements and forecasts for the *BTE* of two datasets, Set-00 and Set-02040. The top graphs indicate that the *BTE* values for Set-00 exhibit a noticeable upward trend, ranging from around 0.24 to 0.36. This suggests a gradual improvement in efficiency over time or during the duration of the experiment. Meanwhile, in Set-02040, the *BTE* values exhibit a broader range of variations, suggesting a higher

diversity of experimental settings or distinct fuel compositions. The lower graphs depict the level of agreement between the model's predictions and the real data, which is very precise in both sets of data. This demonstrates the model's ability to properly represent actual situations by effectively predicting *BTE* values, independent of the cause of the variations. This agreement affirms the dependability and precision of the model in forecasting the thermal efficiency of braking.

Table 10. Comparison of the *BSFC* meaning using experimental data and simulation.

Set-00	Set-02040
	
	

The *BTE* of the engine depends on the generated power, fuel consumption and lower heating value of the fuel. By varying the engine speed, in most cases, the best *BTE* results are obtained when the engine is running at ~70% load (see Table 11). In such cases, sufficient power is generated, and the excess air is sufficient for efficient combustion. Thermal efficiency is better at medium and higher engine speeds (3300 rpm and 3300 rpm) as more power is developed in these cases. When comparing fuel blends, WCO20 has the best BTE values. This is due to the lower heating value of these fuels and their low fuel consumption due to efficient combustion in the event of a sufficient excess of air.

Table 12 displays Pearson's correlation coefficients that evaluate the agreement between projected and actual values for three parameters, *BSFC* and *BTE*, for two datasets: Set-00 and Set-02040. All parameters in both sets have a high correlation coefficient, approaching 1, showing a robust positive link between forecasts and actual values. The surplus air ratio coefficients for the Set-00 kit and the Set-02040 kit are 0.99997 and 0.99995, respectively. The specific fuel consumption for braking is 0.99996 for both kits. The braking thermal efficiency coefficients are 0.99998 and 0.99992 for the two kits, respectively. The strong correlation coefficients demonstrate that the model properly predicted all these factors, affirming its dependability and precision.

Table 11. Comparison of the *BTE* meaning using experimental data and simulation.

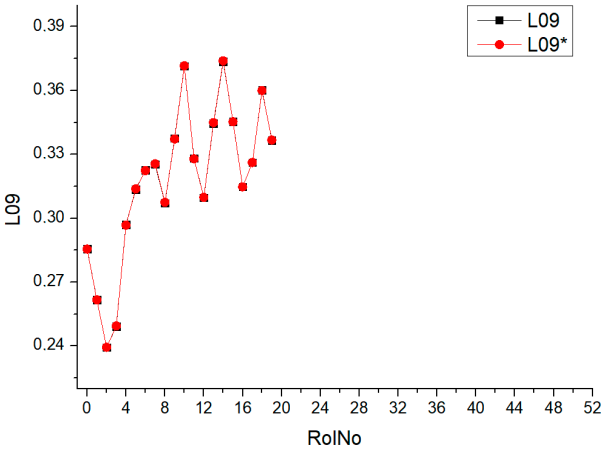
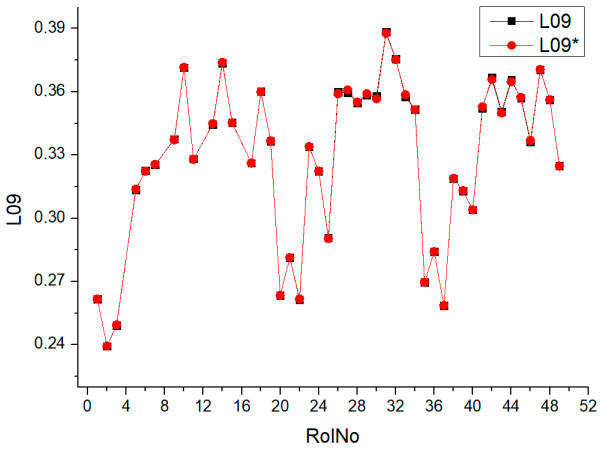
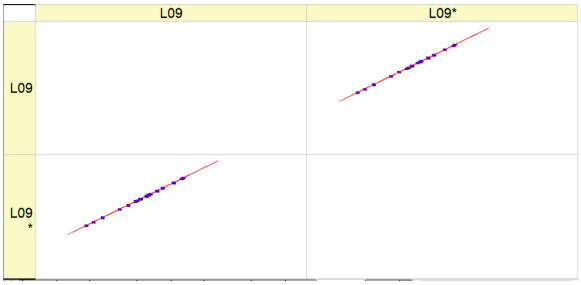
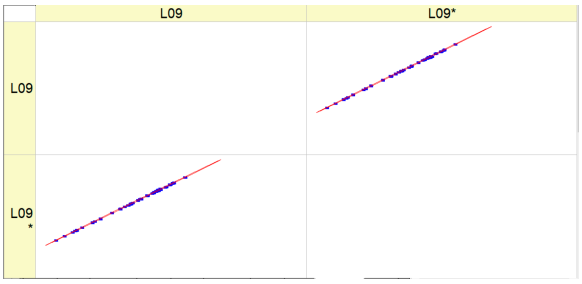
Set-00	Set-02040
	
	

Table 12. Comparison of the Pearson's correlation coefficient of the parameters for both datasets.

Parameter	Dataset 00	Dataset 02040
The excess air ratio (λ)	0.99997	0.99995
Brake specific fuel consumption (*BSFC*), g·kWh^{-1}	0.99996	0.99996
Brake thermal efficiency (*BTE*)	0.99998	0.99992

Although the Pearson correlation coefficient describes the strength of the relationship between the predicted and experimental data, it does not reveal the absolute and relative prediction errors. Therefore, the root mean square error (RMSE) and the mean absolute percentage error (MAPE) were additionally calculated.

RMSE allows us to assess the extent of absolute deviations in the scale of the original measurement units, while MAPE provides a relative error estimate, allowing us to compare the prediction accuracy of different parameters. As can be seen from Table 13, low RMSE and MAPE values were obtained for all main energy parameters, confirming that the ANN model is characterized not only by a very strong correlation but also by low absolute and relative prediction errors.

It should be noted that the higher MAPE value in the case of BTE (L09) is related to the numerical representation of the scale used, not to the prediction inaccuracy. The errors of the normalized BTE indicator (L08) remain small; therefore, it should be considered the main criterion for assessing the accuracy of BTE.

Table 13. Comparison of the Pearson's correlation coefficient of the parameters for both datasets.

Parameter	Symbol	RMSE	MAPE (%)
Excess air ratio	λ (L06)	0.0060	1.15
Brake specific fuel consumption	BSFC (L07), $g \cdot kWh^{-1}$	2.41	0.70
Brake thermal efficiency (normalized)	BTE (L08), –	0.0646	1.12
Brake thermal efficiency (non-normalized)	BTE (L09)*	2.09×10^7	24.21

5. Discussion

Figure 3 displays three quasilinear graphs illustrating the distribution of Pearson correlation coefficients for three parameters: BSFC, BTE, and λ. The upper graph illustrates a declining trend in the Pearson correlation coefficient as the percentage of WCO rises. The coefficient first stands at about 1.0000 for diesel fuel, denoting a very robust association, and thereafter declines to roughly 0.9997 for WCO40, showing a little less strong but still significant link. The center graph shows a marginal rise in the Pearson correlation coefficient from diesel to WCO20, followed by a decline while transitioning to WCO40. This pattern demonstrates a very robust association across all fuel types, but with a somewhat diminished correlation for the WCO40 mixture. The lower graph exhibits a similar pattern to the BSFC graph, as seen by the decreasing Pearson correlation coefficient from diesel to WCO40. The coefficient remains very high, surpassing 0.9992, showing a robust association. However, the correlation is somewhat weaker for WCO40 in comparison to diesel and WCO20.

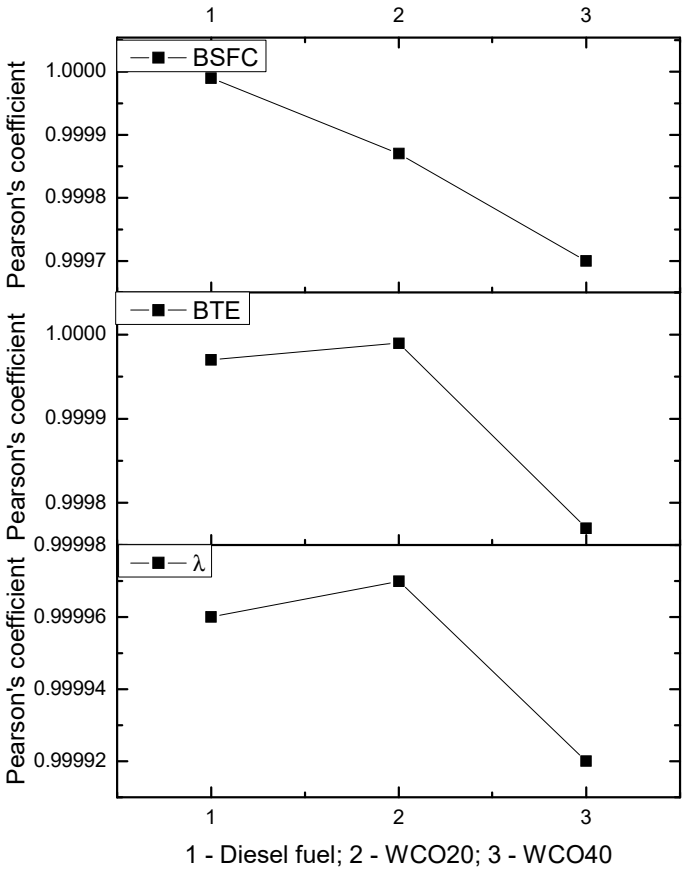


Figure 3. Pearson's correlation coefficients for engine performance parameters across different fuel mixtures.

The observed slight decrease in the Pearson correlation coefficient with increasing WCO concentration is not a random phenomenon and should not be interpreted as an unreliability of the modeling method. On the contrary, this effect reflects the complexity of the combustion process with the use of a larger proportion of alternative fuel mixtures.

As the WCO concentration increases, the main physicochemical properties of the fuel, such as density, viscosity, lower calorific value, oxygen content and carbon–hydrogen ratio, change. These changes have a direct impact on the quality of spraying, fuel–air mixture formation and ignition delay, which leads to greater cycle-to-cycle variability in the combustion phase [43].

WCO-containing mixtures have higher molecular heterogeneity compared to standard diesel, which makes combustion kinetics more sensitive to local fluctuations in temperature, pressure and mixture composition. The literature notes that such conditions often lead to higher dispersion of heat release rate and ignition delay, especially at partial loads [44].

This dispersion of the combustion process directly affects the relationship between input and output parameters, so statistical correlation indices, such as the Pearson coefficient, may decrease slightly even with a physically correct model. Thus, the decrease in correlation at higher WCO concentrations does not indicate combustion instability in the classical sense, but more complex and nonlinear combustion processes caused by fluctuations in fuel properties [49].

In view of this, the ability of the artificial neural network to maintain high prediction accuracy even with these complex processes confirms that the model properly captures the trends determined by combustion physics, not just statistical relationships.

The data indicate that the relationships between these metrics remain robust across all fuel types, although they marginally diminish as the quantity of waste cooking oil in the fuel rises. This may indicate alterations in the uniformity of engine functionality and forecasts of emissions while using elevated levels of WCO.

6. Conclusions

1. This research used an artificial neural network model that showed a remarkable ability to accurately forecast three crucial parameters: *BSFC* and *BTE*. The predicted values closely aligned with the actual values of these parameters. Pearson correlation coefficients over 0.999 indicated a high level of reliability and accuracy for the model.
2. The examination of datasets Set-00 and Set-02040 revealed a pronounced correlation between the predicted and actual values in both sets. However, the larger variability observed in Set-02040 can be attributed to a wider range of experimental conditions, including variations in fuel mixtures and different experimental settings.
3. The Set-00 dataset showed a rising trend in *BTE*, suggesting that changes in experimental settings or fuel mixture modifications may have had a role in efficiency improvement.
4. The analysis of *BSFC* revealed a decline in Set-00, suggesting that experiments or model applications may have contributed to improved fuel efficiency, resulting in a reduction in total fuel consumption.
5. The study's findings validate the applicability of the artificial neural network model in predicting the parameters of internal combustion engines. This indicates that such models can effectively be utilized to enhance engine performance, minimize emissions, and improve fuel efficiency across various experimental conditions or with different fuel compositions.
6. Both the experimental study and the neural network prediction have shown that the best energy performance of a compression ignition engine can be achieved at medium engine speeds and ~70% load using the WCO20 fuel mixture.

Author Contributions: Conceptualization, J.M., A.R., A.G., O.C. and E.R.; methodology, J.M., A.R., A.G., O.C. and E.R.; software, J.M. and A.G.; validation, J.M., A.R., A.G., O.C. and E.R.; formal analysis, J.M. and A.G.; investigation, J.M., A.R., A.G., O.C. and E.R.; resources, J.M., A.R., A.G., O.C. and E.R.; data curation, J.M., A.R., A.G., O.C. and E.R.; writing—original draft preparation, J.M., A.R. and A.G.; writing—review and editing, J.M., A.R., A.G., O.C. and E.R.; visualization, J.M., A.R., A.G., O.C. and E.R.; supervision, J.M.; project administration, J.M.; funding acquisition, J.M., A.R. and A.G. All authors have read and agreed to the published version of the manuscript.

Funding: This research received no external funding.

Data Availability Statement: The data presented in this study are available on request from the corresponding author.

Conflicts of Interest: The authors declare no conflicts of interest.

References

1. Bereczky, A. The Past, Present and Future of the Training of Internal Combustion Engines at the Department of Energy Engineering of BME. In *Proceedings of the Vehicle and Automotive Engineering*; Jarmai, K., Bollo, B., Eds.; Springer International Publishing: Cham, Switzerland, 2017; pp. 225–234.
2. Hunicz, J.; Mikulski, M.; Shukla, P.C.; Gęca, M.S. Partially Premixed Combustion of Hydrotreated Vegetable Oil in a Diesel Engine: Sensitivity to Boost and Exhaust Gas Recirculation. *Fuel* **2022**, *307*, 121910. [CrossRef]
3. Das, A.; Rokhum, S.L. Renewable Diesel and Biodiesel: A Comparative Analysis. In *Renewable Diesel*; Elsevier: Amsterdam, The Netherlands, 2024; pp. 123–166.
4. Diesel Fuel and Exhaust Emissions (EHC 171, 1996). Available online: https://www.inchem.org/documents/ehc/ehc/ehc171.htm (accessed on 31 July 2024).
5. Caban, J.; Vrabel, J.; Górnicka, D.; Nowak, R.; Jankiewicz, M.; Matijošius, J.; Palka, M. Overview of Energy Harvesting Technologies Used in Road Vehicles. *Energies* **2023**, *16*, 3787. [CrossRef]
6. Kozłowski, E.; Zimakowska-Laskowska, M.; Wiśniowski, P.; Šnauko, B.; Laskowski, P.; Laskowski, J.; Matijošius, J.; Świderski, A.; Torok, A. Analysis of Instantaneous Energy Consumption and Recuperation in Electric Buses During SORT Tests Using Linear and Neural Network Models. *Energies* **2025**, *18*, 5107. [CrossRef]
7. Kozłowski, E.; Zimakowska-Laskowska, M.; Dudziak, A.; Wiśniowski, P.; Laskowski, P.; Stankiewicz, M.; Šnauko, B.; Lech, N.; Gis, M.; Matijošius, J. Analysis of Instantaneous Energy Consumption and Recuperation Based on Measurements from SORT Runs. *Appl. Sci.* **2025**, *15*, 1681. [CrossRef]
8. Warguła, Ł.; Kukla, M.; Lijewski, P.; Dobrzyński, M.; Markiewicz, F. Influence of Innovative Woodchipper Speed Control Systems on Exhaust Gas Emissions and Fuel Consumption in Urban Areas. *Energies* **2020**, *13*, 3330. [CrossRef]
9. Matušinec, J.; Hrabec, D.; Šomplák, R.; Nevrlý, V.; Pecha, J.; Smejkalová, V.; Redutskiy, Y. Cooking Oil and Fat Waste Management: A Review of the Current State. *Chem. Eng. Trans.* **2020**, *81*, 763–768. [CrossRef]
10. Fuc, P.; Lijewski, P.; Sokolnicka, B.; Siedlecki, M.; Szymlet, N. Analysis of Exhaust Gas Flow Through a Particulate Filter in the Exhaust of the Spark Ignition Direct Injection Engine. In *AIP Conference Proceedings*; AIP Publishing LLC.: Melville, NY, USA, 2019; Volume 2078.
11. Kozłowski, E.; Rimkus, A.; Zimakowska-Laskowska, M.; Matijošius, J.; Wiśniowski, P.; Traczyński, M.; Laskowski, P.; Madlenak, R. Energy and Environmental Impacts of Replacing Gasoline with LPG Under Real Driving Conditions. *Energies* **2025**, *18*, 5522. [CrossRef]
12. Vekateswarulu, T.C.; Raviteja, C.; Vidya Prabhakar, K.; Dulla, J.; Reddy, A.; Mikkili, I.; Venkatanarayana, A. A Review on Methods of Transesterification of Oils and Fats in Bio-Diesel Formation. *Int. J. ChemTech Res.* **2014**, *6*, 974–4290.
13. Aatola, H.; Larmi, M.; Sarjovaara, T.; Mikkonen, S. Hydrotreated Vegetable Oil (HVO) as a Renewable Diesel Fuel: Trade-off between NOx, Particulate Emission, and Fuel Consumption of a Heavy Duty Engine. *SAE Int. J. Engines* **2008**, *1*, 1251–1262. [CrossRef]
14. Payri, F.; Molina, S.; Martín, J.; Armas, O. Influence of Measurement Errors and Estimated Parameters on Combustion Diagnosis. *Appl. Therm. Eng.* **2006**, *26*, 226–236. [CrossRef]
15. Han, Z.; Reitz, R.D. Turbulence Modeling of Internal Combustion Engines Using RNG κ-ε Models. *Combust. Sci. Technol.* **1995**, *106*, 267–295. [CrossRef]
16. Chakraborty, A.; Roy, S.; Banerjee, R. An Experimental Based ANN Approach in Mapping Performance-Emission Characteristics of a Diesel Engine Operating in Dual-Fuel Mode with LPG. *J. Nat. Gas Sci. Eng.* **2016**, *28*, 15–30. [CrossRef]

17. Gul, M.; Shah, A.N.; Aziz, U.; Husnain, N.; Mujtaba, M.A.; Kousar, T.; Ahmad, R.; Hanif, M.F. Grey-Taguchi and ANN Based Optimization of a Better Performing Low-Emission Diesel Engine Fueled with Biodiesel. *Energy Sources Part Recovery Util. Environ. Eff.* **2022**, *44*, 1019–1032. [CrossRef]
18. Niu, X.; Yang, C.; Wang, H.; Wang, Y. Investigation of ANN and SVM Based on Limited Samples for Performance and Emissions Prediction of a CRDI-Assisted Marine Diesel Engine. *Appl. Therm. Eng.* **2017**, *111*, 1353–1364. [CrossRef]
19. Bhowmik, S.; Paul, A.; Panua, R.; Ghosh, S.K.; Debroy, D. Performance-Exhaust Emission Prediction of Diesosenol Fueled Diesel Engine: An ANN Coupled MORSM Based Optimization. *Energy* **2018**, *153*, 212–222. [CrossRef]
20. Borucka, A.; Kozłowski, E.; Parczewski, R.; Antosz, K.; Gil, L.; Pieniak, D. Supply Sequence Modelling Using Hidden Markov Models. *Appl. Sci.* **2022**, *13*, 231. [CrossRef]
21. Gholamian, E.; Seyed Mahmoudi, S.M.; Balafkandeh, S. Techno-Economic Appraisal and Machine Learning-Based Gray Wolf Optimization of Enhanced Fuel Cell Integrated with Stirling Engine and Vanadium-Chlorine Cycle. *Int. J. Hydrog. Energy* **2024**, *51*, 1227–1241. [CrossRef]
22. Selech, J.; Joachimiak-Lechman, K.; Klos, Z.; Kulczycka, J.; Kurczewski, P. Life Cycle Thinking in Small and Medium Enterprises: The Results of Research on the Implementation of Life Cycle Tools in Polish SMEs—Part 3: LCC-Related Aspects. *Int. J. Life Cycle Assess.* **2014**, *19*, 1119–1128. [CrossRef]
23. Tuan Hoang, A.; Nižetić, S.; Chyuan Ong, H.; Tarelko, W.; Viet Pham, V.; Hieu Le, T.; Quang Chau, M.; Phuong Nguyen, X. A Review on Application of Artificial Neural Network (ANN) for Performance and Emission Characteristics of Diesel Engine Fueled with Biodiesel-Based Fuels. *Sustain. Energy Technol. Assess.* **2021**, *47*, 101416. [CrossRef]
24. Borucka, A.; Wiśniowski, P.; Mazurkiewicz, D.; Świderski, A. Laboratory Measurements of Vehicle Exhaust Emissions in Conditions Reproducing Real Traffic. *Measurement* **2021**, *174*, 108998. [CrossRef]
25. Burdzik, R. Novel Method for Research on Exposure to Nonlinear Vibration Transferred by Suspension of Vehicle. *Int. J. Non-Linear Mech.* **2017**, *91*, 170–180. [CrossRef]
26. Castresana, J.; Gabiña, G.; Martin, L.; Basterretxea, A.; Uriondo, Z. Marine Diesel Engine ANN Modelling with Multiple Output for Complete Engine Performance Map. *Fuel* **2022**, *319*, 123873. [CrossRef]
27. Uslu, S. Optimization of Diesel Engine Operating Parameters Fueled with Palm Oil-Diesel Blend: Comparative Evaluation between Response Surface Methodology (RSM) and Artificial Neural Network (ANN). *Fuel* **2020**, *276*, 117990. [CrossRef]
28. Nor, C.M.; Mamat, R.; Najafi, G.; Yasin, M.M.; Ihsan, C.; Noor, M. Prediction of Marine Diesel Engine Performance by Using Artificial Neural Network Model. *J. Mech. Eng. Sci.* **2016**, *10*, 1917–1930. [CrossRef]
29. Selech, J.; Rogula-Kozłowska, W.; Piątek, P.; Walczak, A.; Pieniak, D.; Bondaronok, P.; Marcinkiewicz, J. Failure and Reliability Analysis of Heavy Firefighting and Rescue Vehicles: A Case Study. *Eksploat. Niezawodn.–Maint. Reliab.* **2023**, *26*. [CrossRef]
30. Jeon, M.; Noh, Y.; Shin, Y.; Lim, O.-K.; Lee, I.; Cho, D. Prediction of Ship Fuel Consumption by Using an Artificial Neural Network. *J. Mech. Sci. Technol.* **2018**, *32*, 5785–5796. [CrossRef]
31. Yusaf, T.F.; Buttsworth, D.R.; Saleh, K.H.; Yousif, B.F. CNG-Diesel Engine Performance and Exhaust Emission Analysis with the Aid of Artificial Neural Network. *Appl. Energy* **2010**, *87*, 1661–1669. [CrossRef]
32. Ahmad, M.W.; Mourshed, M.; Rezgui, Y. Trees vs Neurons: Comparison between Random Forest and ANN for High-Resolution Prediction of Building Energy Consumption. *Energy Build.* **2017**, *147*, 77–89. [CrossRef]
33. Cirak, B.; Demirtas, S. An Application of Artificial Neural Network for Predicting Engine Torque in a Biodiesel Engine. *Am. J. Energy Res.* **2014**, *2*, 74–80. [CrossRef]
34. Bizon, K.; Continillo, G.; Lombardi, S.; Mancaruso, E.; Vaglieco, B.M. ANN-Based Virtual Sensor for On-Line Prediction of In-Cylinder Pressure in a Diesel Engine. In *Computer Aided Chemical Engineering*; Elsevier: Amsterdam, The Netherlands, 2014; Volume 33, pp. 763–768.
35. Kökkülünk, G.; Akdoğan, E.; Ayhan, V. Prediction of Emissions and Exhaust Temperature for Direct Injection Diesel Engine with Emulsified Fuel Using ANN. *Turk. J. Electr. Eng. Comput. Sci.* **2013**, *21*, 2141–2152. [CrossRef]
36. Selvaraj, R.; Moorthy, I.G.; Kumar, R.V.; Sivasubramanian, V. Microwave Mediated Production of FAME from Waste Cooking Oil: Modelling and Optimization of Process Parameters by RSM and ANN Approach. *Fuel* **2019**, *237*, 40–49. [CrossRef]
37. Tütüncü, K.; Allahverdi, N. Modeling the Performance and Emission Characteristics of Diesel Engine and Petrol-Driven Engine by ANN. In *Proceedings of the International Conference on Computer Systems and Technologies and Workshop for PhD Students in Computing*; ACM: Ruse, Bulgaria, 2009; pp. 1–6.
38. Oğuz, H.; Sarıtas, I.; Baydan, H.E. Prediction of Diesel Engine Performance Using Biofuels with Artificial Neural Network. *Expert Syst. Appl.* **2010**, *37*, 6579–6586. [CrossRef]
39. Carbot-Rojas, D.A.; Escobar-Jiménez, R.F.; Gómez-Aguilar, J.F.; Téllez-Anguiano, A.C. A Survey on Modeling, Biofuels, Control and Supervision Systems Applied in Internal Combustion Engines. *Renew. Sustain. Energy Rev.* **2017**, *73*, 1070–1085. [CrossRef]
40. Vom Lehn, F.; Brosius, B.; Broda, R.; Cai, L.; Pitsch, H. Using Machine Learning with Target-Specific Feature Sets for Structure-Property Relationship Modeling of Octane Numbers and Octane Sensitivity. *Fuel* **2020**, *281*, 118772. [CrossRef]

41. López-Flores, F.J.; Rubio-Castro, E.; Ponce-Ortega, J.M. Incorporating Machine Learning for Thermal Engines Modeling in Industrial Waste Heat Recovery. *Chem. Eng. Res. Des.* **2022**, *181*, 239–252. [CrossRef]
42. Žvirblis, T.; Hunicz, J.; Matijošius, J.; Rimkus, A.; Kilikevičius, A.; Gęca, M. Improving Diesel Engine Reliability Using an Optimal Prognostic Model to Predict Diesel Engine Emissions and Performance Using Pure Diesel and Hydrogenated Vegetable Oil. *Eksploat. Niezawodn.–Maint. Reliab.* **2023**, *25*. [CrossRef]
43. Wu, G.; Ge, J.C.; Choi, N.J. A Comprehensive Review of the Application Characteristics of Biodiesel Blends in Diesel Engines. *Appl. Sci.* **2020**, *10*, 8015. [CrossRef]
44. How, H.G.; Masjuki, H.H.; Kalam, M.A.; Teoh, Y.H. Influence of Injection Timing and Split Injection Strategies on Performance, Emissions, and Combustion Characteristics of Diesel Engine Fueled with Biodiesel Blended Fuels. *Fuel* **2018**, *213*, 106–114. [CrossRef]
45. Karpanai Selvan, B.; Das, S.; Chandrasekar, M.; Girija, R.; John Vennison, S.; Jaya, N.; Saravanan, P.; Rajasimman, M.; Vasseghian, Y.; Rajamohan, N. Utilization of Biodiesel Blended Fuel in a Diesel Engine—Combustion Engine Performance and Emission Characteristics Study. *Fuel* **2022**, *311*, 122621. [CrossRef]
46. Loo, D.L.; Teoh, Y.H.; How, H.G.; Teh, J.S.; Andrei, L.C.; Starčević, S.; Sher, F. Applications Characteristics of Different Biodiesel Blends in Modern Vehicles Engines: A Review. *Sustainability* **2021**, *13*, 9677. [CrossRef]
47. Palani, Y.; Devarajan, C.; Manickam, D.; Thanikodi, S. Performance and Emission Characteristics of Biodiesel-Blend in Diesel Engine: A Review. *Environ. Eng. Res.* **2020**, *27*, 200338. [CrossRef]
48. Zhang, Z.; Li, J.; Tian, J.; Dong, R.; Zou, Z.; Gao, S.; Tan, D. Performance, Combustion and Emission Characteristics Investigations on a Diesel Engine Fueled with Diesel/Ethanol/n-Butanol Blends. *Energy* **2022**, *249*, 123733. [CrossRef]
49. Geng, P.; Cao, E.; Tan, Q.; Wei, L. Effects of Alternative Fuels on the Combustion Characteristics and Emission Products from Diesel Engines: A Review. *Renew. Sustain. Energy Rev.* **2017**, *71*, 523–534. [CrossRef]
50. Gruodis, Alytis VALLUM01. Advanced Tool for Implementation of Artificial Neural Network Containing Tabular Interface for Input/Output. Available online: https://cris.mruni.eu/cris/entities/person/alytisgruodis/publications (accessed on 14 April 2023).
51. Geofrey, N. Implementing Neural Networks from Scratch: A Step-by-Step Guide. 2024. Available online: https://www.articsledge.com/post/perceptron (accessed on 14 April 2023).
52. Matijošius, J.; Rimkus, A.; Gruodis, A. Validation Challenges in Data for Different Diesel Engine Performance Regimes Utilising HVO Fuel: A Study on the Application of Artificial Neural Networks for Emissions Prediction. *Machines* **2024**, *12*, 279. [CrossRef]
53. Matijošius, J.; Rimkus, A.; Gruodis, A. Prediction of the main environmental and energy characteristics of diesel engines using an artificial neural network for pure diesel fuel, pure HVO, and a mixture of these fuels in the ratio 50/50 by volume. *Transp. Probl.* **2024**, *19*, 69–82. [CrossRef]
54. Matijošius, J.; Rimkus, A.; Gruodis, A. Validation of Ecology and Energy Parameters of Diesel Exhausts Using Different Fuel Mixtures, Consisting of Hydrogenated Vegetable Oil and Diesel Fuels, Presented at Real Market: Approaches Using Artificial Neural Network for Large-Scale Predictions. *Machines* **2024**, *12*, 353. [CrossRef]
55. Sonawane, S. Understanding and Implementing Neural Networks in Java from Scratch. Available online: https://github.com/SuyashSonawane/JavaNet (accessed on 31 December 2023).

Disclaimer/Publisher's Note: The statements, opinions and data contained in all publications are solely those of the individual author(s) and contributor(s) and not of MDPI and/or the editor(s). MDPI and/or the editor(s) disclaim responsibility for any injury to people or property resulting from any ideas, methods, instructions or products referred to in the content.